THE EFFECTS OF LUBRICATION ON THE ROLLING CONTACT SURFACE DEFORMATION

By:

FOO CHUN YIT

(Matrix no.: 131143)

Supervisor:

Dr. Nurul Farhana Binti Mohd Yusof

May 2019

This dissertation is submitted to
Universiti Sains Malaysia
As partial fulfilment of the requirement to graduate with honors degree in
BACHELOR OF ENGINEERING (MECHANICAL ENGINEERING)

School of Mechanical Engineering
Engineering Campus
Universiti Sains Malaysia

DECLARATION

This work has not previously been accepted in substance for any degree and is not being concurrently submitted in candidature for any degree.

Signed……（FOO CHUN YIT）

Date …….

STATEMENT 1

This thesis is the result of my own investigations, except where otherwise stated. Other sources are acknowledged by giving explicit references. Bibliography/references are appended.

Signed……（FOO CHUN YIT）

Date …….

STATEMENT 2

I hereby give consent for my thesis, if accepted, to be available for photocopying and for interlibrary loan, and for the title and summary to be made available to outside organizations.

Signed……（FOO CHUN YIT）

Date …….

ACKNOWLEDGEMENT

Firstly, I would like to express my deepest gratitude to my research supervisor, Dr. Nurul Farhana Binti Mohd Yusof for her patient guidance and enthusiastic encouragement of this research. The advices and assistance provided by her keeping my progress on schedule and runs smooth.

I would also like to extend my thanks to the assistance engineers of workshop for their help in giving guidelines in fabricating the equipment required for the research and giving me advices on conducting the experiments. Especially, I would like to thank Mr. Baharom to assist me on fabricating the motor base plate and help me remove the inner race bearing from the shaft. Besides, I also want to say thank you to Mr. Ashamuddin to help me to do surface scanning for inner race bearing using Alicona IFM machine.

Finally, I would like to express my great appreciation to my friends for their valuable and informative suggestions during the planning and development of this research work. Especially I would like to thank my friend, Tan Sak Jie because he always helps me to switch off the AC motor when I am not free. Voon Zhen Liang is one of my friends who I want to say thank you to. This is because we share to use the IMC device, but he always allows me to use first.

TABLE OF CONTENTS

LIST OF FIGURES

LIST OF TABLES

LIST OF SYMBOLS

H_{min}	Minimum film thickness
U	Speed parameter
G	Material parameter
W	Load parameter
λ	Lambda ratio
η_o	Absolute viscosity
u_o	Surface velocity
E’	Effective modulus of elasticity
R	Radius of curvature
ε	Material coefficient
F	Load per length
Rq_1	Root-Mean-Square of surface roughness of inner race
Rq_2	Root-Mean-Square of surface roughness of roller
V_1	Poisson’s ratio of material of inner race
V_2	Poisson’s ratio of material of roller
E_1	Young modulus of material of inner race
E_2	Young modulus of material of roller
R_1	Radius of inner race
R_2	Radius of roller
M	Mass of load
g	Gravitational acceleration

L	Length of roller
R_a	Average surface roughness
R_q	Root-Mean-Square surface roughness
R_{sk}	Skewness
R_{ku}	Kurtosis
Rmr_1	Material ratio 1
Rmr_2	Material ratio 2

LIST OF ABBREVIATIONS

2D	Two Dimensional
3D	Three Dimensional
RMS	Root-Mean-Square
IFM	Infinite Focus Microscope
IMC	Intelligent Management Center

ABSTRAK

Pelinciran memainkan peranan penting untuk mencegah atau mengurangkan geseran di antara dua permukaan. Dalam sentuhan berguling, pelincir membentuk lapisan atau filem untuk memisahkan permukaan berguling dan untuk menahan beban yang dikenakan. Pelinciran yang tidak mengcukupi biasanya menyebabkan perubahan bentuk permukaan yang teruk dan kehausan dan menggalakkan jangka hayat operasi yang pendek. Dalam kerja ini, kesan pelinciran terhadap perubahan bentuk permukaan berguling telah dikaji dengan menguunakan galas penggelek silinder. Dua kaji telah dijalankan untuk membandingkan perubahan bentuk permukaan galas penggelek kering dan galas penggelek dengan pelincir. Galas kering dikendalikan oleh motor AC dengan 1500 rpm, kekasaran permukaan perlumbaan dalaman diukur setiap 30 minit sehingga gagal. Bagi galas pelincir, kekasaran permukaan perlumbaan dalaman diukur setiap 10 jam sehingga jam ke-100 dicapai. Paras getaran diukur pada permulaan dan penghujung eksperimen. Analisis topografi permukaan dan profil menggerutu menunjukkan perubahan bentuk permukaan berlaku dengan teruk pada galas tanpa pelinciran yang mana alur lubang kecil telah terbentuk dan terdapat pengumpulan zarah-zarah bahan yang dibuang pada permukaan. Untuk galas dengan pelinciran, perubahan bentuk permukaan adalah sedikit dan dijangkakan pelincir gris berkemampuan untuk menyingkirkan zarah-zarah tersebut dan mengelakkan mereka daripada terkumpul di permukaan. Selain itu, galas kering rosak dan percikan api berlaku pada minit ke-105 manakala galas pelincir masih beroperasi dengan lancar selepas berputar selama 100 jam. Ini menunjukkan bahawa pelincir memanjangkan jangka hayat galas dengan cekap. Parameter ketebalan filem pelinciran kepada kekasaran rms telah diperolehi menggunakan persamaan Hamrock-Dawson menunjukkan galas dengan pelincir gris beroperasi dengan $\lambda = 0.3$ iaitu pelinciran sempadan. Untuk analisis kekasaran permukaan, kekasaran permukaan RMS dan kurtosis permukaan gegelang dalam dengan pelincir adalah lebih rendah berbanding dengan permukaan gegelang dalam kering. Permukaan gegelang dalam pelincir mempunyai nilai pencongan negatif yang rendah manakala permukaan gegelang dalam kering mempunyai nilai pencongan positif yang tinggi. Analisis getaran menunjukkan bahawa pelinciran dapat mengurangkan getaran pada galas. Tanpa pelinciran, paras getaran sangat tinggi ketika galas gagal iaitu

1.71 m/s^2 manakala hanya 0.32 m/s^2 paras getaran diperolehi selepas beroperasi selama 100 jam dengan pelinciran.

ABSTRACT

Lubrication plays an important role to prevent or reduce friction between two surfaces. In rolling contact, the lubricant forms a layer of film to separate the rolling surfaces and to sustain the applied load. Insufficient lubrication normally results in severe surface deformation and wear promoting short operation life. In this work, the effects of lubrication on the rolling surface contact deformation were studied using cylindrical roller bearing. Two sets of experiments were carried out to compare the surface deformation of a dry roller bearing and a lubricated roller bearing. The dry bearing was run by an AC motor with 1500 rpm, the surface roughness of inner race was measured every 30 minutes until it failed. Whereas for lubricated bearing, the surface roughness of inner race was measured by every 10 hours until 100th hour was reached. Vibration level was measured at the beginning and at the end of experiments. The surface topography and surface asperities profile analysis results show that the surface deformation is severe for un-lubricated dry bearing where small micro pitting groove was formed and there is an accumulation of removed material particles on the surface. For the lubricated bearing, surface deformation is very low and it is expected that the grease has a capability to remove the particles and avoided them from accumulating on the surface. Besides, the dry bearing was damaged and sparks occurred at 105th minutes while lubricated bearing was still operating smoothly after rotating for 100 hours. This showed that lubricant prolonged the life span of the bearing efficiently. The lubrication film thickness over root mean square roughness parameter (λ) is determined by the Hamrock-Dowson equation which showed that the grease lubricated bearing operated at $\lambda = 0.3$ which is under boundary lubrication. For surface roughness analysis, it is observed that the RMS surface roughness and kurtosis of the lubricated inner race were lower as compared to the surface of dry inner race. The surface of lubricated inner race had low negative skewness value while surface of the dry inner race has high positive skewness value. From RMS vibration acceleration level analysis, it is observed that the lubricant managed to reduce the vibration of the bearing. Without lubrication, the vibration level is very high during bearing failure which is at 1.71 m/s^2 while only 0.32 m/s^2 of vibration level was obtained after 100 hours of operation in lubricated condition.

CHAPTER 1 INTRODUCTION

In this section, brief introduction on the research on the effect of lubricant on the rolling contact surface deformation is discussed.

1.1 Research Background

Road vehicle tyres, metro wheels, ball bearing, cam and followers are the general components which work with rolling elements. When they are rolling, they generate rolling contact forces which are transferred to a rolling contact area between the rolling elements. Rolling contact is a point or line where two rolling or rotating elements touch each other. However, defect or deformations often occurs at the rolling contact surfaces. Consequently, the component will be damaged due to the defects or deformations.

Cylindrical roller bearing is an example of rolling-element bearing which transmit forces between shaft and housing. The bearing uses rollers to maintain the separation between the bearing races. As the inner bearing race rotates due to the movement of shaft, it causes the rollers rotating too. Since the rollers are rotating, it can reduce the friction and make the shaft to rotate smoothly. In addition, Rotational friction and support radial and axial loads can be reduced using roller bearing.

Figure 1.1 Roller bearing

However, defects such as inner raceway defects, outer raceway defects and roller defects can be caused by the waviness of the rolling element and the surface roughness and the friction on the rolling surface contacts which depends on the state of lubrication. Waviness is an error in form caused by incorrect geometry of the process producing the surface. Contact force and friction loss can be changed by the surface waviness of bearing. While the surface roughness are the surface irregularities that appear as a consequence of the process if it is carried out on a geometrically perfect machine. Even though the rollers look smooth and well-polished, the surface is not truly smooth on a microscopic scale. Under a microscope, we can see that the surface of a smooth material is actually rough and sharp. Besides, we can see a lot of peaks and valleys on the surface. The random deviation of peaks and valleys is the surface roughness.

When two rolling contact surfaces are rotating, plastic deformation and wear occur at the contact points due to friction. As mentioned earlier that both bearing ring, rollers and races are not perfectly smooth. Resonances and high vibrations can be caused by the defects. For example, when the number of rolling elements and the number of waves is same, it can lead to severing vibrations. As another example, the outer race waviness causes roller dynamic unbalance. Hence, it affects the cage's motion and a severe vibration is induced when the rolling element passage frequency or one of its harmonics coincides with a natural frequency. Making it clear, when the outer race of bearing vibrates, the surface of the bearing will keep on moving up and down through the upper limit, start point and lower limit as shown in the Figure 1.2. The repeated movement of the surface is called vibration and consists of its own frequency which is the number of completed cycles within a specific period of time. If the bearing's frequency is equal to the natural frequency which is the frequency at which a system oscillates when not subjected to a continuous or repeated external force, resonance will occur and causes the bearing to break down and fail. Therefore, the effects of the rolling contact surface deformation must be studied carefully.

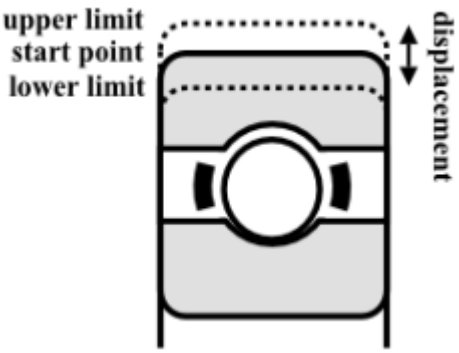

Figure 1.2 Vibration of bearing

Lubricant is a liquid that reduces the friction between two contact surfaces. The lubricant film thickness may reduce when the surfaces are moving or rotating. Furthermore, it can transmit forces, transport foreign particles, and help in heating or cooling the rolling contact surfaces. Thus, lubricant is one of the effective methods that can be used to minimize the rolling contact surface deformation. Lubricant can be in oil form like engine oil or grease. Different oil lubricants have different viscosity values which can have different effects on the surfaces. For example, when a low viscosity oil lubricant is used, the surfaces undergo relative motion, the lubricant will spill out of the gap between the two surfaces and hence will not serve the purpose if the application does not permit the repetitive lubrication. With very high viscosity oil lubricant, there would be power losses in friction. Hence, oil lubricant viscosity should be selected depending on the type of application. Grease is another type of lubricant which is in the form of film or semisolid. It consists of base oil and thickener in its structure and is normally used in bearing to possess a high initial viscosity where shear is applied. The difference between oil and grease is that grease is applied at the place where oil cannot stay in position and it can be used to seal gap to prevent seep of water. Grease is selected based on its base oil properties due to its complex composition. However, it may face starvation when the bearing is rotated, and this can affect the formation of film and the effectiveness of lubrication.

Stribeck curve is widely used to describe the relationship between lubrication parameter and coefficient of friction. In the curve, it is divided into three regions. They are boundary lubrication, elastohydrodynamic lubrication and hydrodynamic

lubrication as shown in Figure 1.3. In boundary lubrication, there is no hydrodynamic pressure and no pressure is built up in the lubrication due to the speed of rotating of the rolling element is very slow. Hence, only a thin film of lubricant is formed, and the loading is carried by the asperities at the contact points. With increasing speed, the lubricant is transported into the space between the surfaces. The upward forces of the lubricant push the surfaces apart. The further the surfaces are pushed apart, the lower the friction. In elastohydrodynamic lubrication, hydrodynamic pressure exists in the lubricant and the loading is carried by both hydrodynamic pressure and contact pressure at the contact points. In this region, lubricant manages to reduce the friction to minimum level and hence reduce the damage to the bearing. In hydrodynamic lubrication, the rolling elements are fully separated by the film of lubrication when the speed increases. However, the internal friction of the lubricant increases, and thus the friction of the entire system increases. De Laurentis and Goncalves had finished a study to show that the friction curve for grease has a great difference from the Stribeck curve. However, Kanazawa's research shows that the grease friction curve is similar to Stribeck curve. Therefore, experiments are carried out to study the effects of lubricants on the rolling contact surface deformation and vibration generated.

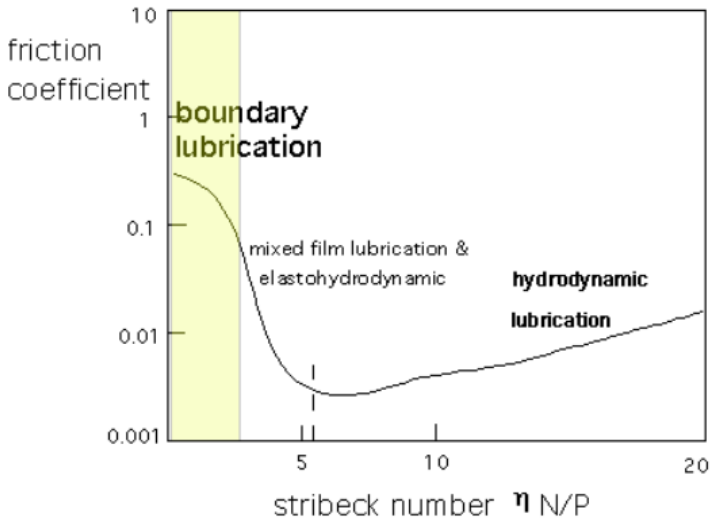

Figure 1.3 Stribeck Curve (Kanazawa, Sayles, & Kadiric, 2017)

1.2 Objectives

1. To study the effect of the lubrication on the rolling contact surface deformation.
2. To investigate the effect of surface deformation on the vibration level

1.3 Problem Statements

Smooth rolling contact surface is very important to the roller bearings, cams and followers and other components which involve two rotating elements. However, the surface is not smooth on a microscopic value because of asperities on the surface of rolling bodies. However, researchers did not consider the changes of the asperities while studying the rolling contact surface condition. The asperities will deform due to wear after every cycle of rotation. This wear and deformation can cause vibration, noise and cracks, and lead to failure of the rolling bodies and also reduce the efficiency and life span of the components. Lubrication plays an important role to form a layer to separate two rolling or sliding surfaces and to sustain the applied load. Insufficient lubrication can influence the surface characteristics and vibration level. There is a need to identify the effect of lubrication on the surface condition particularly at the asperity level to improve the life span of the components which involve two rolling elements.

1.4 Scope of Project

In this project, cylindrical roller bearing is chosen to be used in experiment because it has rolling contact surface when the rollers and inner raceway are rolling. There are two type of bearing condition tested in this study, there are dry condition without lubrication and lubricated condition. Since grease is used in most of the rolling element bearings as a lubricant, so grease is the only lubricant to be used in this study. The surface deformation is measured from the beginning of the experiment until damaged. Surface characterization is performed to evaluate the surface condition, and the surface roughness and asperities are plotted. The lubrication regime related to minimum film thickness and surface roughness are identified using Hamrock Dowson equation. The surface roughness of roller is assumed to be constant from the beginning of the experiment until the end because removing the roller from the bearing may damage the bearing. The vibration level produced by the surface deformation is evaluated too.

CHAPTER 2 LITERATURE REVIEW

In this section, relevant resources are reviewed in order to obtain sufficient knowledge about rolling contact surface deformation, wear, lubrication and vibration.

2.1 Rolling Contact Surface Deformation

According to El-Thalji and Jantunen (El-Thalji & Jantunen, 2014), the evolution of rolling contact wear and surface topology features occurs in five stages. They are running-in stage, steady stage, defect initiation stage, defect propagation stage and damage growth stage as shown in Figure 2.1. In the running-in stage, the material at the contact points will be worn out and transferred from the peaks of the asperities to valleys. Therefore, the surface of the rolling element at the end of the stage will be smoother. Since the roughness of the surface becomes smoother, the steady stage is characterized by uniform film lubrication. In this stage, the topology change is slow because of uniform film lubrication. However, due to sliding and transfer of film lubrication, surface interaction between the roller and bearing occurs and this results in abrasive wear and some contaminants may enter the contact zone and cause vibration and defect or surface dentation is generated. As a result of defect formation, contact force increase and concentrates the applied tangential force. Crack propagation is caused by the increase in tangential force and the friction. However, the shape of the dent is changing over the time, the defect completion is accelerated when the lubricant is transferred into the cracks on the surface. After the material is removed from the surface, new asperity is generated, and the new surface material is not as hard as the material of the original surface. As a result, more dentations are generated to generate more defects on different locations. The crack propagates downward from the surface with inclination until it meets the secondary crack. Then, a large material is detached from the surface and it causes the defect to become larger and the surface to become rougher.

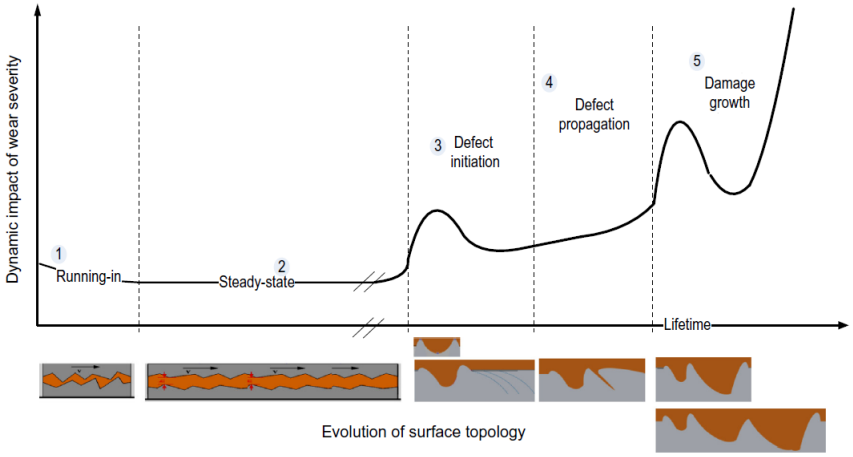

Figure 2.1 Evolution of dynamic behavior and surface topology due to wear evolution (El-Thalji & Jantunen, 2014)

Ismail et al. (R. Ismail, 2010) divided the wear-time behavior into three type: running-in, steady state and wear out as shown in Figure 2.2. During running in, the wear events at a high rate initially, then it reduced to a lower value at the end (Ji-Yi Lin, 1989). The topology of the surface is changing over time. Then, the wear and wear rate are almost constant during the steady state. Due to dynamic loading, fatigue is caused on the surface of material and hence large material is degraded from the surface. Thus, the wear rate increases rapidly during wear out. Besides, the lubrication disturbance and increase in temperature are the factor to cause wear rate to increase rapidly.

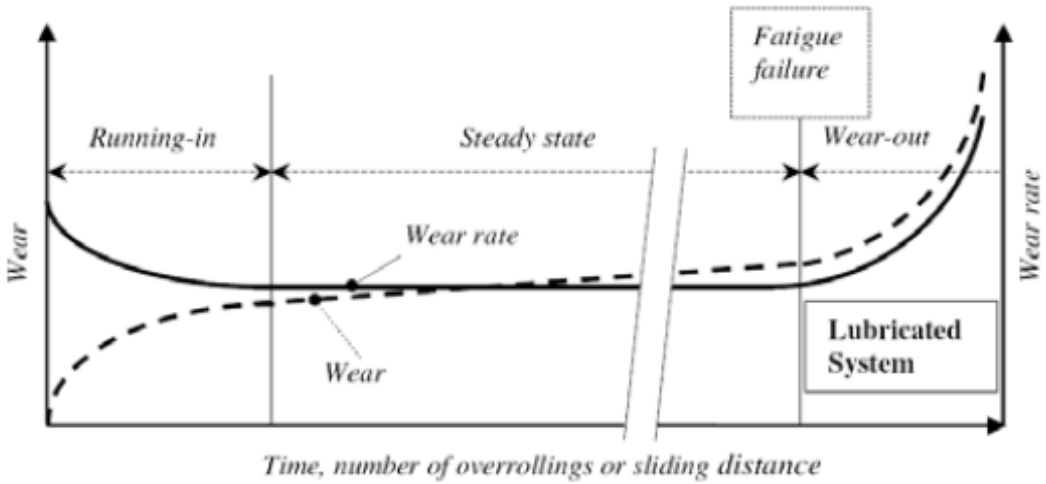

Figure 2.2 Wear and wear rate over time, number of over-rolling or sliding distance (Jamari & Schipper, 2007)

In the figure 2.3, the surface roughness and friction decrease over the time during running in. This is because the change of surface roughness and friction is to minimize the energy flow between the moving surface (Whitehouse, 1980). Then the friction and surface roughness remain almost constant at steady state because of uniform film lubrication.

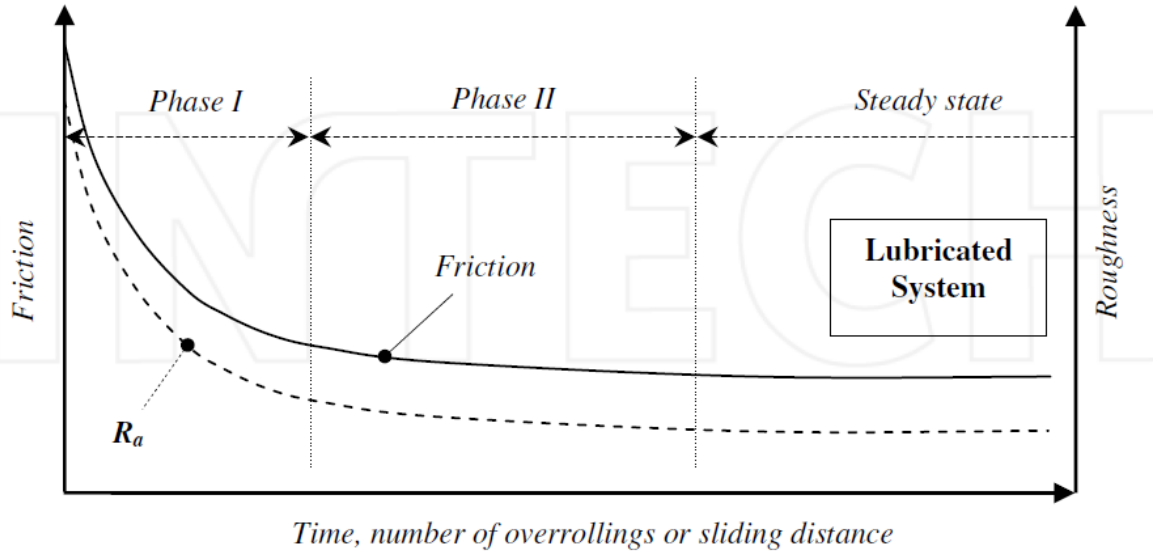

Figure 2.3 Friction and roughness over time, number of over-rolling or sliding distance (Whitehouse, 1980)

However, the researches above do not show how the surface asperities change over the time. It is important to know how the surface asperities change but not only the surface roughness so that we can investigate the relationship between lubrication and surface deformation.

2.2 Regime of Lubrication

2.2.1 Effect of lubricants on Micro-pitting and Wear

Olver and Beveridge (Lainé, Olver, & Beveridge, 2008) constructed the experiments to find the effects of lubricants on micro-pitting wear on the surface of bearing. The micro-pitting experiments were done using three counterface rings and s single roller for each test. For the first experiment, they constructed experiment to find the effect of ZDDP additive with lubricant on the surface deformation. They found that lubricants with ZDDP additive will cause rollers to have significant wear rate as compared to lubricants without ZDDP additive as shown in Figure 2.4.

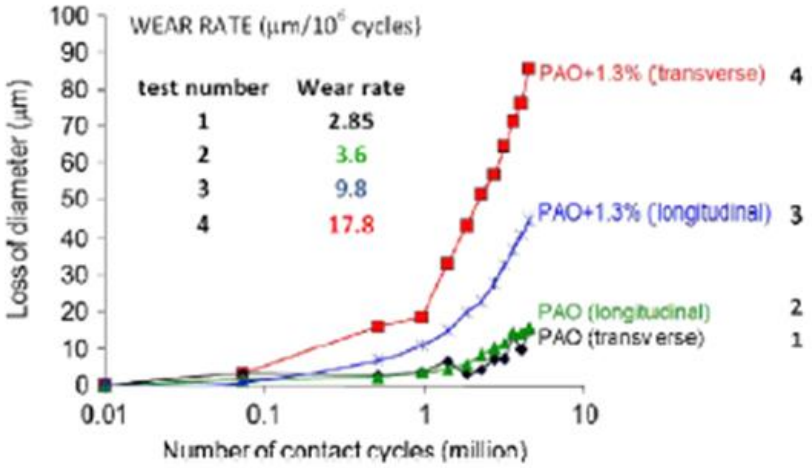

Figure 2.4 Graph of loss of diameter against number of contact cycles (Lainé et al., 2008)

In the second experiment, 4 rollers with different surface roughness were used to carry out experiment to find the effect of surface roughness and lubricants on the wear rate. In the result, they found that roller with lower surface rougher has higher lambda, λ and showed little wear even after full duration of test which spends 5 hours to complete 4.5 million contact cycles. Lambda is used to describe the relationship between the minimum film thickness and surface roughness. They concluded that with higher lambda value, rollers have fewer counterfaces to interact and effect of lubricants will be more significant as shown in Figure 2.5. Besides, the micropitting formation causes severe wear when the Lambda, λ value at 0.12. At 0.12 Lambda value, the film

thickness, micropitting formation and wear influence each other obviously. However, after the Lambda is greater than 0.16, although there are micropittings, there are no severe wear found on the surface of roller.

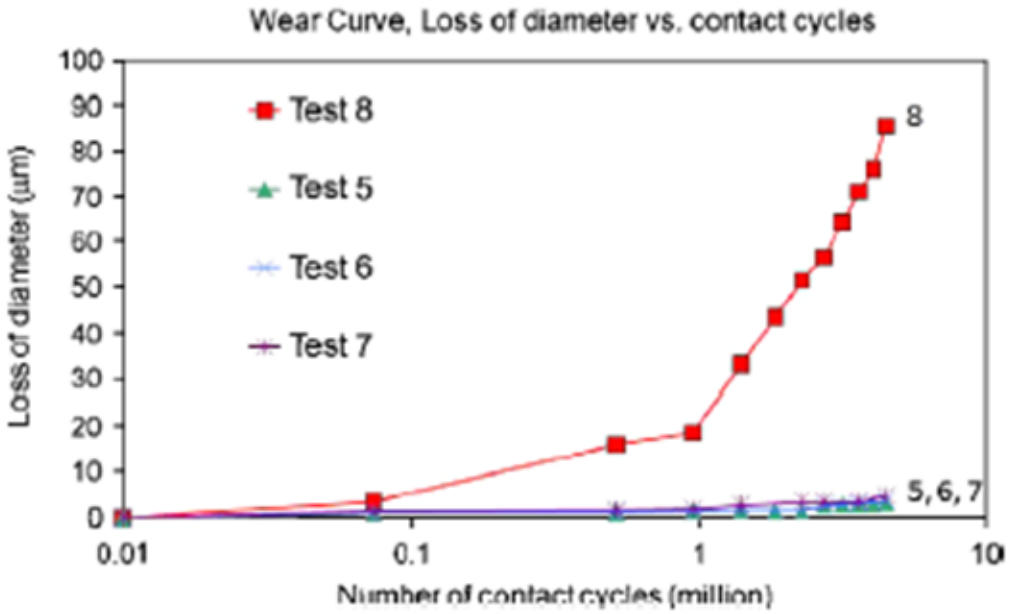

Figure 2.5 Graph of loss of diameter against number of contact cycles (Lainé et al., 2008)

2.2.2 Analysis of the Lubrication Regime

Lubricant film thickness is an important parameter to evaluate the coefficient of friction on the rolling surfaces. As long as the lubricant film is sufficiently thick and resilient enough to prevent asperity–asperity contacts, the coefficient of friction tends to be very low. Analysis of surface parameter and vibration of roller bearing was done by Yusof and Ripin (Mohd Yusof & Ripin, 2014) where surface degradation was monitored and lubricant film thickness inside the roller bearing was calculated to find the relationship between the roughness height and vibration. The minimum film thickness, h_{min} and lambda (minimum film thickness over root mean square roughness parameter using Hamrock and Dowson (Bruce, 2010). The results show that the vibration is depending on the λ. At the lambda value where at λ>3, it is in full-film EHL lubrication and the root mean square vibration level is low as shown in Figure 2.6. The finding shows that lubricant can reduce the vibration level.

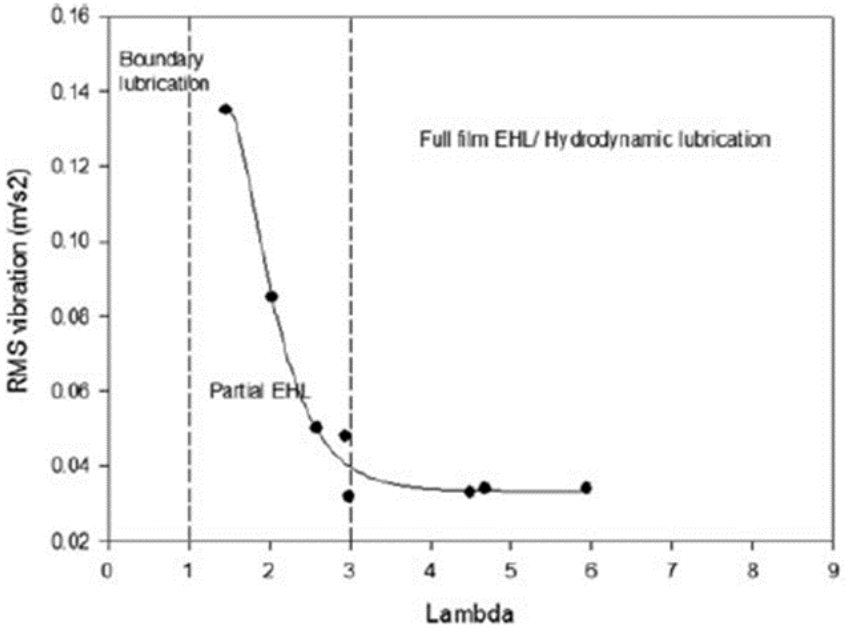

Figure 2.6 Root Mean Square Vibration as a function of λ (Mohd Yusof & Ripin, 2014)

2.3 Rolling Element Bearing Vibration

Bearings were operated in normal state condition and defected condition by Saruhan et al. (Saruhan, Sandemir, Çiçek, & Uygur, 2014) under different shaft running speeds which are 17Hz, 25Hz, 33Hz, and 41Hz. The defected bearing has four different defects such as outer raceway defect, inner raceway defect, ball defect and combination of bearing component defect. The result shows that the defect frequency increases greatly if the bearing has defects. This defect frequencies are very dangerous because it may cause resonance if it is near to natural frequency of the rotating bearing.

Williams et al. (Williams, Ribadeneira, Billington, & Kurfess, 2001) measured the vibration acceleration on the inner race bearing surface and found that inner race of bearing has highest damage as compared to outer race and rolling element. This is because inner race of bearing interacts with rotating shaft which can produce large elastic stress wave. For the inner race acceleration test, the result shows that acceleration increases to a maximum level, then decreases and increases again. The fluctuating acceleration is caused by nature of damage. However, obvious increase in acceleration is visible after 120 running hours as shown in Figure 2.7.

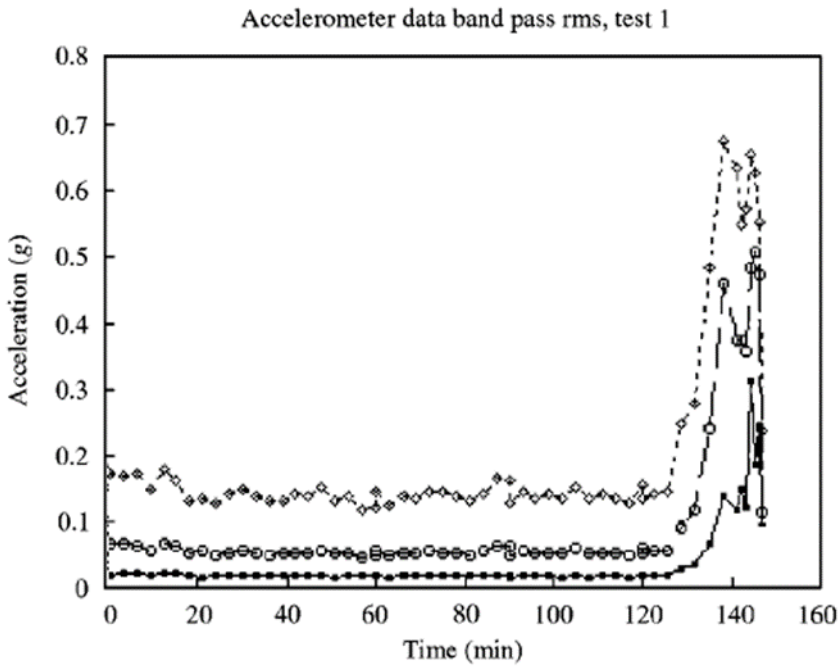

Figure 2.7 Graph of acceleration against time (Williams et al., 2001)

CHAPTER 3 METHODOLOGY

In this chapter, the experiment setup, surface characterization, lubrication regime identification and vibration level measurement are discussed.

3.1 Experiment Set Up

The experiment was carried out using rolling element bearing test rig. The experimental rig consists of cylindrical roller bearings, support bearings, shaft, coupling, AC motor, motor controller and load holder as shown in figure 3.1. The shaft was supported by pillow blocks and driven by AC motor. The speed of rotation of the AC motor was controlled by speed controller. The shaft was set at 1500 rpm and a load of 98 N was given. The load on the bearing was applied with a point contact produced at the bearing housing. Therefore, most of the applied load was concentrated at the middle of the bearing width.

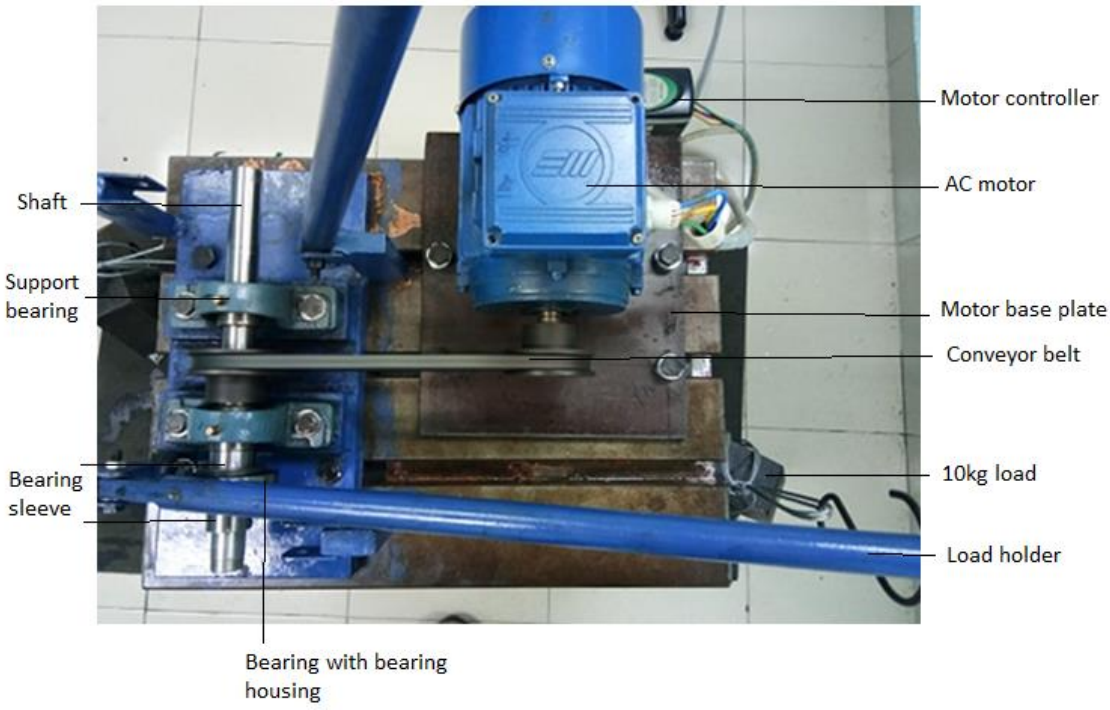

Figure 3.1 Experimental set up

Two cylindrical roller bearings (FAG X-life) were used in this study. The specification of the cylindrical bearing is shown in table 3.1. The cylindrical bearing consists of inner race, outer race, rollers and cage as shown in figure 3.2.

Number of rollers	13
Roller diameter (d_r)	7.5 mm
Roller length (L_r)	9 mm
Inner bore diameter (D_i)	25 mm
Outside ring diameter (D_o)	52 mm
Pitch diameter (d_m)	38.5 mm
Width of bearing (B)	15 mm
Material of roller and inner race	52100 Stainless steel
Poison's ratio (v)	0.3
Young modulus of elasticity (E)	210 GPa
Material coefficient (α)	2.2×10^{-8} m^2/N

Table 3.1 Specification of cylindrical roller bearing

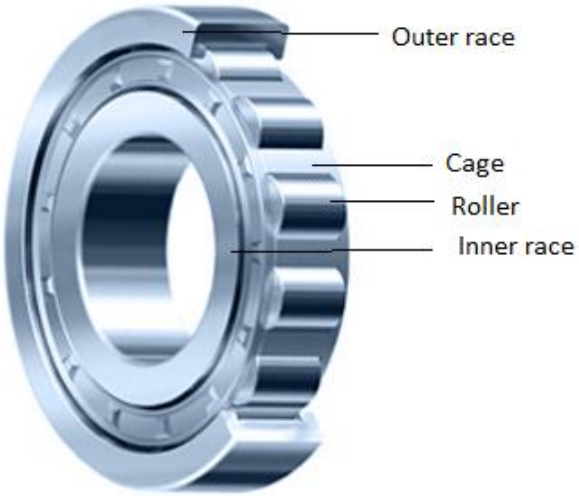

Figure 3.2 Bearing components

3.1.1 Fabrication

In this experiment, some fabrications and experiment set-up needed to be done before conducting the experiment. First, a motor base plate was fabricated so that the AC motor can be fixed on the test rig. A 25 cm x 29 cm x 1 cm mild steel plate was cut using gas welding torch. 4 holes with 12 mm diameter were drilled on the mild steel using drilling machine according to the dimension in figure A-1. 4 holes with 8 mm diameter were drilled on the metal plate according to the dimension in figure A-1. Then, 8.5 mm tap and handle were used to make thread to the 4 holes with 8 mm diameter so that 10mm bolt can be screwed.

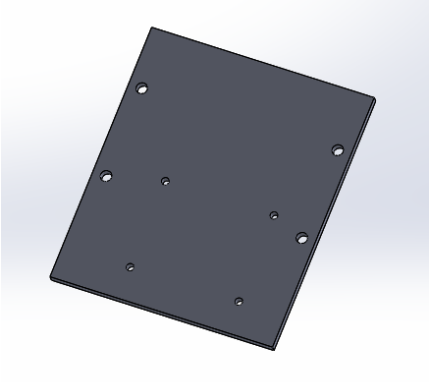

Figure 3.3 SolidWork sketch of motor base plate

The AC motor circuit was connected as shown in the figure 3.4 (a) using phase wires by following the instructions on the AC motor cover in figure 3.4 (b). The 3 phase wires then were connected to the motor controller as shown in figure 3.4 (c).

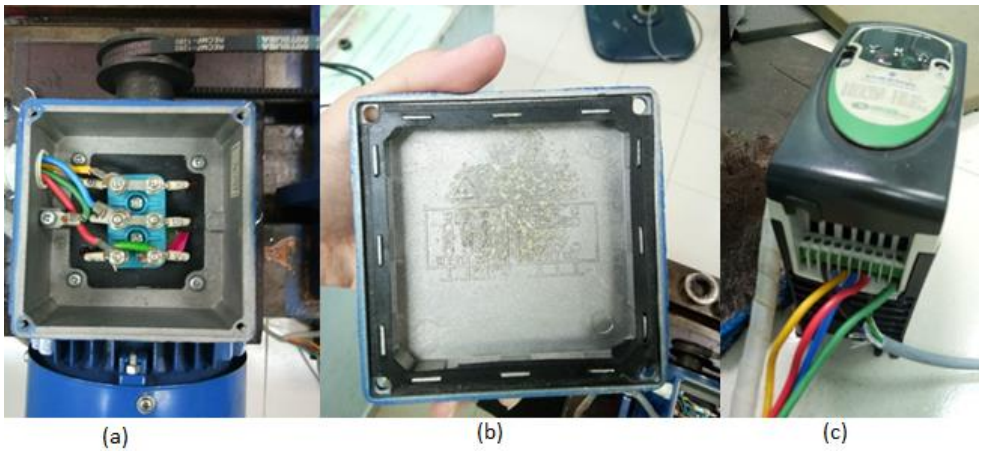

Figure 3.4 (a) Circuit connection of AC motor, (b) circuit connection instruction on cover motor, (c) motor controller circuit connection

The 10kg load was tied using steel rope as shown in figure 3.5 (a) so that it can be hanged on the S hanger to apply 98 N on the bearing. 8 nut locks were fabricated by welding the 4 nuts with 10 mm diameter and 4 nuts with 12mm diameter on 3.4 cm x 8 cm steel plates as shown in figure 3.5 (b). The two supporting bearings with shaft was fixed on the test rig using 4 bolts with 10mm diameter and 4 nut locks with 10mm diameter. The AC motor was fixed on the motor base plate by screwing 4 bolts with 10mm diameter through the motor to the 8.5 mm holes with thread. A conveyor belt was applied to connect the shaft with the AC motor. Then, the position of the AC motor was adjusted until the conveyor belt is parallel to the test rig. 4 bolts and nut locks with 12mm diameters were used to fix the AC motor. Bearing was inserted into bearing housing and locked using alliance key. Then, a bearing sleeve was inserted into the shaft followed by the bearing then followed by another bearing sleeve as shown in figure 3.5 (c). Next, both bearing sleeves were locked by alliance key. The whole experiment set up is shown as figure 3.1.

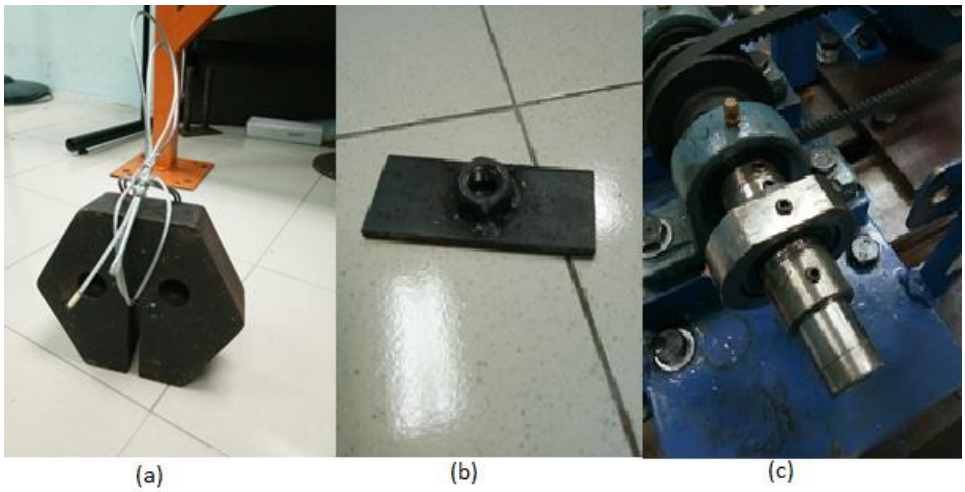

Figure 3.5 (a) 10 kg load tied by steel rope, (b) nut lock, (c) shaft with bearing and bearing sleeves

3.1.2 Experiment Procedures

The apparatus needed was prepared and set up as shown in the figure 3.6 below before the experiment.

Figure 3.6 Apparatus set-up

Both inner race of the two cylindrical roller bearings were taken out and the oil on the surface of the inner races were cleaned using acetone with cloth. A small scratch was made on the outside of the measured area of inner races of bearing using grinder as a reference point as shown in figure 3.7.

Figure 3.7 Reference point marking on the inner race bearing

One of the rollers was removed from the bearings. The surface roughness of the both inner races of bearing and roller of the bearing were measured using Alicona IFM machine. The surface roughness was recorded as the roughness for 0^{th} cycle of rotation. The roller was installed back to the bearing. Then, one of the bearings was dipped into acetone to remove the oil and lubricant inside the bearing. The dry bearing with bearing

housing was installed into the shaft as shown in the figure 3.8 (a). 10 kg load was applied on the S hanger as shown in figure 3.8 (b).

Figure 3.8 (a) installed bearing, (b) load on S hanger

The accelerometer which is connected to IMC device is attached on the housing bearing using wax. A large piece of sponge was placed near the test rig as shown in figure 3.9 to avoid the accelerometer from falling onto the floor while the motor was running.

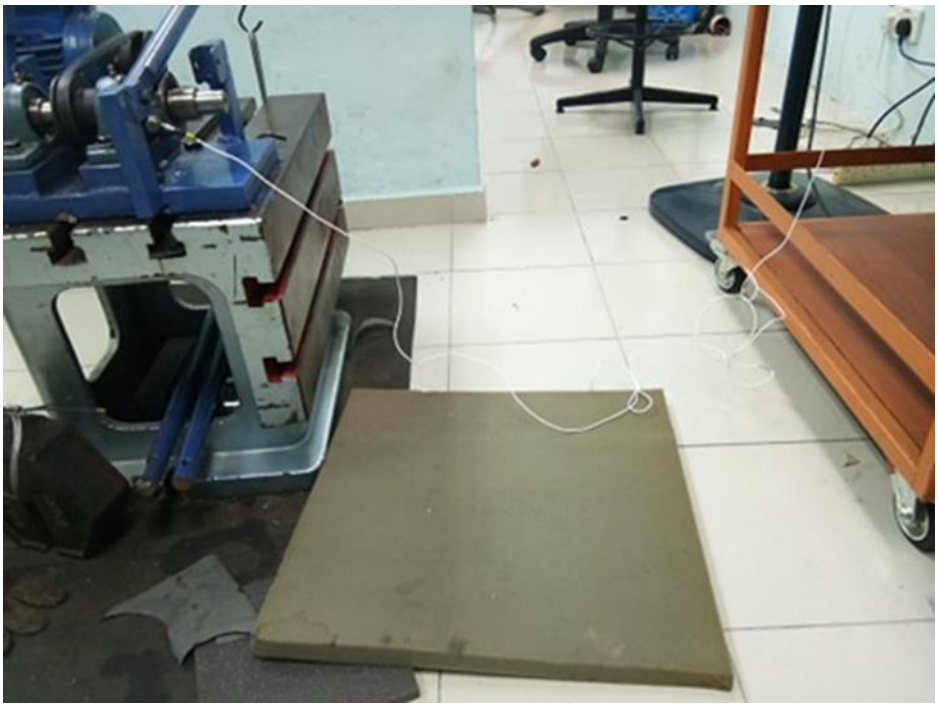

Figure 3.9 A large piece of sponge on floor

Then, the AC motor controller was set to run the motor at 1500 rpm. The vibration level of the bearing is measured using IMC device. After 30 minutes of running, the AC motor was switched off and the bearing is removed from the shaft. By wearing glove, the surface of inner race of the dry bearing was cleaned using acetone. Then, the surface roughness of the inner race was measured again using Alicona IFM machine and the result was recorded as roughness at 1st set of rotation. Then, the shaft was rubbed using sand paper and the bearing was installed to the shaft and run. The roughness was measured every 30 minutes until the bearing failed. After the experiment for dry bearing, another bearing was applied with 0.5ml grease using syringe as shown in figure 3.10 (a) and 3.10 (b).

Figure 3.10 0.5 ml grease

With the same procedure as dry bearing, the lubricated bearing was installed to the shaft and run with 1500 rpm. The vibration level was measured using the IMC device. After 10 hours, the inner race bearing was taken out and cleaned with acetone. The surface roughness was measured using Alicona IFM machine. Then the experiment was repeated for 10 times. All data of surface roughness and vibration level were collected and tabulated.

3.2 Surface Characterization

Alicona Infinite Focus Microscope (IFM) was used for surface roughness characterization as shown in figure 3.11. The surface characterization was performed periodically.

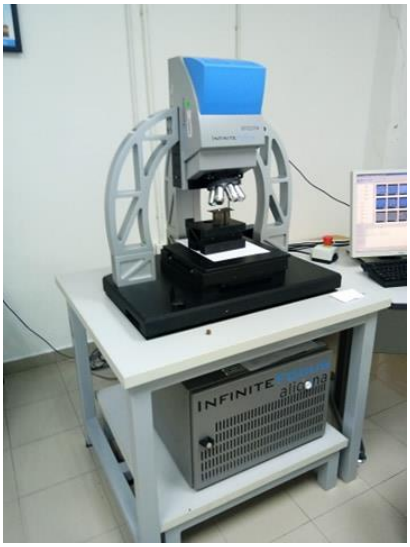

Figure 3.11 Alicona Infinite Focus Microscope machine

The inner race was removed every 30 minutes and 10 hours for dry bearing and lubricated bearing respectively, the inner race was cleaned using acetone and dried using cloth. Then, the surface was scanned at 10X main fraction as shown in figure 3.12. During scanning, the reference mark was identified therefore the scanning can be carried out at the same location periodically.

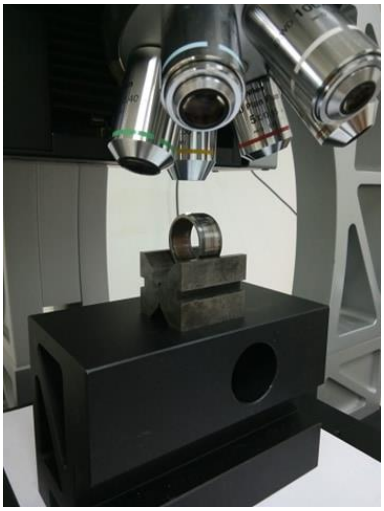

Figure 3.12 Scanning of inner race surface

The brightness of the figure was set until the figure became clear. At the image field, a measured area was selected to be scanned. Start button was pressed to scan the surface of inner race bearing. After finishing scanning, the result and data were saved in a file. The file was opened and a line was selected starting at the scratch and ending at the edge of the bearing for measuring the surface roughness along the line. Then, a measured area was selected on the surface for measuring the surface roughness within that area. Average surface roughness, Root-Mean-Square roughness, Kurtosis, Skewness, and material ratio 1 and 2 were measured and 3D view of the scanned surface was viewed. All the data were recorded in table A-1 and A-2. Definitions of the surface parameters is shown in table 3.2.

Surface Parameter	Definition
Average surface roughness, R_a	The average height of ordinates of the surface measured from the mean line regardless of the sign within the sampling length. $R_a = \frac{h_1 + h_2 + h_3 + h_4 + h_5 + \ldots\ldots + h_n}{n} = \frac{\sum_{i=1}^{n} h_i}{n}$
RMS surface roughness, R_q	The square root of the mean of the square of the ordinates of the surface measured from the mean line over one sampling length. $R_z = \sqrt{\frac{h_1^2 + h_2^2 + h_3^2 + \ldots. + h_n^2}{n}}$
Skewness, R_{sk}	Used to measure the symmetry of the surface roughness profile about the mean line. $R_{sk} = \frac{1}{nR_q^3} \sum_{i=1}^{n} y_i^3$

Kurtosis, R_{ku}	Used to measure the sharpness of the roughness distribution and describe the shape of the profile. $R_{ku} = \frac{1}{nR_q^4}\sum_{i=1}^{n} y_i^4$
Material ratio 1, Rmr_1	The fraction of surface which consists of peaks above the core material.
Material ratio 2, Rmr_2	The fraction of surface which will carry the load.

Table 3.2 Definition of surface parameters

3.3 Lubrication Regime Identification

In this study, the bearings were tested in unlubricated and lubricated conditions. For unlubricated condition, the whole bearing was cleaned and submerged into acetone to remove oil. The lubricated bearing was wetted by grease and relubrication was carried out periodically when the bearing was remount after surface scanning. The grease used is SKF LGMT 2/0.4 and the specification is shown in table 3.3.

Brand of grease	LGMT 2/0.4
Base oil type	Mineral
Soap type	Lithium
Base of viscosity 40 °C 100 °C	 110 mm²/s 11 mm²/s
Operating temperature range	–30 to +120 °C
Absolute viscosity (η_o)	0.09 Ns/m^2
DIN 51825 code	K2K-30
Colour	Red Brown

Table 3.3 Specifications of grease

The lubricant film thickness and lubrication regime is determined based on Bruce, R.W modified equations (Bruce, 2010). The equation for minimum film thickness, H_{min} is shown below:

$$H_{min} = 1.714U^{0.0694}G^{0.568}W^{-0.128}R \qquad (1)$$

Where

$$\text{Speed parameter } U = \frac{\eta_o u_0}{E\prime R} \qquad (2)$$

$$\text{Material parameter } G = \varepsilon E' \qquad (3)$$

$$\text{Load parameter } W = \frac{F}{E\prime R} \qquad (4)$$

$$\text{Lambda } \lambda = \frac{h_{min}}{\sqrt{R_{q1}^2 + R_{q2}^2}} \qquad (5)$$

Where

H_{min} is minimum film thickness, U is speed parameter, G is material parameter, W is load parameter, λ is Lambda, η_o is absolute viscosity, u_o is surface velocity, E' is effective modulus of elasticity, R is radius of curvature, ε is material coefficient, F is Load per length, R_{q1} is the root-mean-square surface roughness of inner race bearing and R_{q2} is the root-mean-square surface roughness of roller.

The surface velocity, u_o can be calculated as shown in the equations below:

$$u_o = \frac{u_1 + u_2}{2} \qquad (6)$$

$$u_1 = \frac{2\pi R_1 N}{60} \qquad (7)$$

$$u_2 = \frac{2\pi R_2 N}{60} \qquad (8)$$

Where

U_1 is the surface velocity of bearing, U_2 is the surface velocity of roller, R_1 is the radius of inner race bearing, R_2 is the radius of roller, and N is the motor speed.

Effective modulus of elasticity, E' can be calculated as shown in the equation below (Bruce, 2010):

$$\frac{1}{E'} = \frac{1}{2}\left[\frac{1 - V_1^2}{E_1} + \frac{1 - V_2^2}{E_2}\right] \qquad (9)$$

Where

V_1 is the poisson's ratio of the material of inner race bearing, V_2 is the poisson's ratio of the material of roller, E_1 is the young modulus of the material of inner race bearing and E_2 is the young modulus of the material of roller.